

## Quantitative Characterization of Dislocation Structure coupled with Electromigration in a Passivated Al (0.5wt% Cu) Interconnects

R.I. Barabash<sup>1</sup>, N. Tamura<sup>2</sup>, B.C. Valek<sup>3</sup>, R. Spolenak<sup>4</sup>, J.C. Bravman<sup>3</sup>, G.E. Ice<sup>1</sup> and J.R. Patel<sup>2</sup>

<sup>1</sup> Metals & Ceramics Divisions, Oak Ridge National Laboratory, Oak Ridge TN 37831

<sup>2</sup> Lawrence Berkeley National Laboratory, 1 Cyclotron Road, Berkeley CA 94720

<sup>3</sup> Dept. Materials Science & Engineering, Stanford University, Stanford CA 94305

<sup>4</sup> Max Planck Institut für Metallforschung, Heisenbergstrasse 3, D-7056 Stuttgart, Germany

### ABSTRACT

New synchrotron x-ray microbeam methodology is used to analyze and test the reliability of interconnects. The early stage of plastic deformation induced by electromigration before any damages become visible has been recently revealed by white beam scanning X-ray microdiffraction during an accelerated test on Al interconnect lines. In the present paper, we provide a quantitative analysis of the dislocation structure generated in several micron-sized Al grains in both the middle region and ends of the interconnect line during an *in-situ* electromigration experiment. We demonstrate that the evolution of the dislocation structure during electromigration is highly inhomogeneous and results in the formation of randomly distributed geometrically necessary dislocations as well as geometrically necessary boundaries. The orientation of the activated slip systems and rotation axis depends on the position of the grain in the interconnect line. The origin of the observed plastic deformation is considered in view of constraints for dislocation arrangements under applied electric field during electromigration. The coupling between plastic deformation and precipitation in the Al (0.5% wt. Cu) is observed for the grains close to the anode/cathode end of the line.

### INTRODUCTION

The decrease of interconnect lines dimensions with a simultaneous increase in current density to 1 MA/cm<sup>2</sup> has imposed tremendous challenges for materials and reliability of interconnects. Electromigration depletes material at the cathode end of the interconnect line and causes accumulation near the anode end<sup>1</sup>. Electromigration-induced failure in metal interconnect constitutes a major reliability problem in the semiconductor industry<sup>2</sup>. While the general mechanism of electromigration is understood<sup>3</sup>, the effect of the atomic flow on the local metallic line microstructure is largely unknown. White beam X-ray microdiffraction<sup>4-14</sup> was used to probe microstructure in interconnects<sup>4,11-14</sup> and has recently unambiguously unveiled the plastic nature of the deformation induced by mass transport during electromigration in Al(Cu) lines<sup>15</sup> even before macroscopic damage occurs. The first quantitative analysis of dislocation structure in a grain in the polycrystalline region of the interconnect line was performed in<sup>16,17</sup> and it was shown that

in that region of the interconnect line the dislocations with their lines almost parallel to the current flow direction are formed first. Recent study of precipitation in Al (Cu) interconnects<sup>18</sup> indicates that Cu is preferentially depleted from the cathode end of the line. Analysis of alloying effects in electromigration<sup>19</sup> demonstrates that a complete understanding of why the addition of Cu results in the great improvement of electromigration resistance of Al-based interconnect lines has not been achieved yet.

The aim of the present paper is to understand the complex dislocation structure arising from electromigration-induced plastic deformation in different regions (including the ends) of interconnect lines and to find the possible correlation between Cu drift, precipitation and formation of dislocations.

## EXPERIMENTAL DETAILS

Data collection has been carried out at the X-ray microdiffraction end station on beamline 7.3.3. at the Advanced Light Source. The sample is a patterned Al(0.5% wt. Cu) line (length:30  $\mu\text{m}$ , width 4.1  $\mu\text{m}$ , thickness 0.75  $\mu\text{m}$ ) sputter deposited on a Si wafer and buried under a glass passivation layer (0.7  $\mu\text{m}$  thick). Electrical connections to the line are made through unpassivated Al(Cu) pads connected to the sample by W vias. In the present paper, we concentrate on the evolution of the diffraction pattern of four particular grains (Grains A and E, size:  $\sim 2.5 \mu\text{m}$ ) situated approximately half-way between the middle of the line and the anode end and grains F and G close to the opposite ends of the line. Details on the experimental setting and data collection can be found elsewhere<sup>4-6</sup>. A qualitative description and semi-quantitative interpretation of the entire data set collected for the present sample can be found in a recent article<sup>15</sup>. Orientation maps obtained from the x-ray microdiffraction scans reveal that the grain structure of the line has a random in-plane orientation and a pronounced (111) fiber texture. Only one or a few grains span the width of the line (near bamboo configuration). Grains A and E are in a region of the line, where multiple grains are found transverse to the line, grains F and G are almost at the ends of the line (Fig.1). Dislocation structure was determined from the Laue images by simulating the shape of the reflections observed in the experimental data. Custom software allows us to determine the orientation of the predominant dislocation network in each sample subgrain<sup>16,17, 20</sup>. Here we extended this method to consider gradients with depth in density of randomly distributed geometrically necessary dislocations (GNDs) within the scattering domains separated by geometrically necessary dislocation boundaries (GNBs) and to include the strain gradient parameters.

## RESULTS AND DISCUSSION

### Grains in the middle polycrystalline region of the interconnect line

Before electromigration all Laue patterns show sharp reflections for all grains (Figs.1a,b,c,d (spot1)) and pronounced streaking of the Laue reflections in the majority of Al grains after electric current flow (Figs 1 a,b,c,d (spot5)). The average streaking direction for the grains in the middle of the line is approximately transverse to the length of the line (Fig.1a,b) [Note: this is generally true for the majority of the grains in the lines

except a few of them at the ends] and almost parallel to it close to the end of the lines (Fig. 1c,d). During the first 20 hours, grain F is close to the anode end of the line (Fig. 1c, spots 1-3), which becomes the cathode end after current reversal (Fig. 1c, spots 4,5), and grain G is in the opposite location.

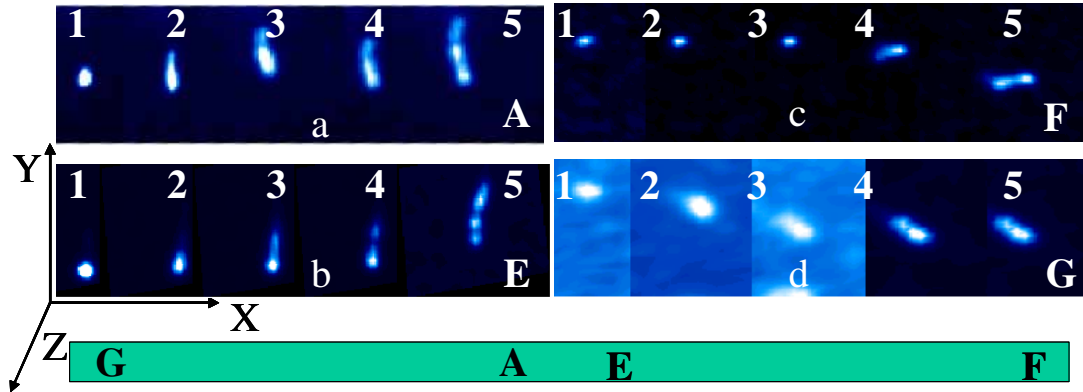


**Figure.1** Change of experimental streaking of (222) Laue spots for A and E grains in the middle of the line (a,b) and for F and G grains (c,d) close to the opposite ends of the interconnect line. The sample was maintained at a constant temperature of 205 °C (1) and the current density was progressively ramped up to 0.98 MA/cm<sup>2</sup> and maintained at this value for a period of 20 hours (2,3). The direction of the current was then reversed for a total period of 19 hours. 1)initial state before the current flow; 2)5 hours; 3)11 hours;4)9 hours reversed current; 5)10 hours reversed current.

The intensity profiles along the streak at different times during the electromigration process are presented in Fig. 2 for grains F, G and E in the reciprocal space in sample basis. For the grain labeled E (in the middle of the line) continuous streaks are observed near all Laue spots in the first measurements made at 0.98 MA/cm<sup>2</sup>. Although the in-plane orientation of the grain E differs from the grain A, the evolution of Laue spots with time of current flow is similar to the one observed for grain A<sup>15-17</sup>. After 14 hours of current flow intensity distribution of the (222) Laue spot becomes asymmetric with strong maximum of the intensity on one side and long weak tail. The orientation of the primary unpaired dislocations corresponds to a Burgers vector  $\mathbf{b} = [\bar{1}10]$  and a dislocation line direction  $\tau = [11\bar{2}]$  and is almost parallel to the direction of the current flow in that grain. After 6 additional hours at the same current density, the intensity distribution in grains A and E breaks into two distinct maxima (Fig.2c, curve 3) indicating that the dislocation structure partially relaxed with the formation of a geometrically necessary boundary (GNB). The density of unpaired boundary dislocations is about  $0.25 \cdot 10^{10} \text{ cm}^{-2}$ . The FWHM<sub>ξ</sub> along the streak direction within each maximum again increased (Fig.2c, curve 3). The density of unpaired individual dislocations within each scattering domain at this stage is equal to  $n^+ = 0.3 \cdot 10^{10} \text{ cm}^{-2}$  (Fig.2c). We then reversed the direction of the current flow to -0.98 MA/cm<sup>2</sup> and after 6 hours the randomly distributed dislocation population decreases, while the portion of dislocations grouping within the GNB increased (Fig.2c, curve 4). This indicates that the opposite direction of the current may “cure” some part of randomly distributed unpaired individual dislocations. The density of unpaired individual dislocations within each scattering domain slightly decreases to  $n^+ =$

$0.2 \times 10^{10} \text{ cm}^{-2}$ . However, the dislocations being grouped into a sub-boundary form a very stable arrangement, which is not destroyed by the opposite direction of the current. After 10 hours with  $J = -0.98 \text{ MA/cm}^2$  a second sub-boundary is formed. The streak splits into three distinct maximums (Figs.2c, curve 5). The second geometrically necessary boundary creates misorientation of  $0.4^\circ$ . The total density of boundary dislocations within the above two boundaries is equal to  $0.6 \times 10^{10} \text{ cm}^{-2}$ . It should be noted that orientation of the secondary slip system in both grain A<sup>17</sup> and grain E is slightly inclined to the direction of the current flow.

### Grains in the near anode/cathode regions of the interconnect line

Grains F and G (Figs.1c,d and Figs. 2a,b) in the opposite ends of the interconnect line show a distinct behavior compared to the grains A and E in the middle of the line. Grain F in the beginning of the experiment is close to the anode end of the line. There is absolutely no increase in the  $\text{FWHM}_\xi$  indicating the absence of plastic deformation in this grain during this period of current flow (more over the FWHM in all directions of the spot even slightly decreases). After the current reversal the grain F becomes close to the cathode end of the line and its  $\text{FWHM}_\xi$  along the streak immediately increases demonstrating high activity of plastic deformation. The density of geometrically necessary dislocations becomes equal  $n^+ = 0.3 \times 10^{10} \text{ cm}^{-2}$ . The orientation of the primary unpaired dislocations corresponds to a Burgers vector  $\mathbf{b} = [\bar{1}01]$  and a dislocation line direction  $\tau = [1\bar{2}1]$  (Fig.3 left) and is almost perpendicular to the direction of the current flow. Next 10 hours of the current flow in the same direction result in the grouping of dislocations within a GNB. Grain G demonstrates the opposite behavior (Figs. 1d,2b).

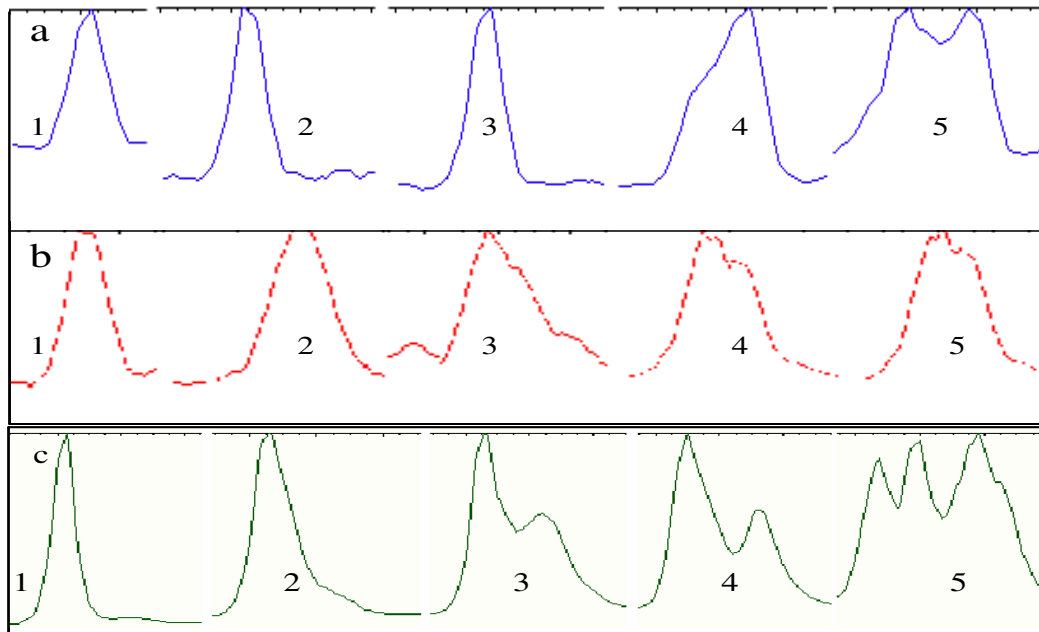


**Figure.2** Intensity distribution along the streak for grains F (a), G (b) located near the opposite ends of the interconnect line and grain E (c) in the middle of the interconnect

line with time of current flow:1)initial state before the current flow; 2)5 hours; 3)11 hours;4)9 hours reversed current; 5)19 hours reversed current.

In the beginning of the experiment it is located close to the cathode end of the line, and immediately since the current is on, the  $\text{FWHM}_\xi$  of Laue streak starts to increase. Opposite to E and F grains the (222) Laue spot in G grain first broadens symmetrically (Fig.2b, curve2). After 6 additional hours at the same current density, the intensity distribution becomes highly asymmetric (with intensity maximum on one side of the streak and long tail of decreasing intensity) and corresponds to dislocation density equal  $n^+ = 0.4 \cdot 10^{10} \text{ cm}^{-2}$  (Fig.2b, curve3). After current reversal the  $\text{FWHM}_\xi$  of the streak slightly decreases and intensity distribution breaks into two distinct maxima (Fig.2b, curve 4) indicating that the dislocation structure partially relaxed with the formation of a geometrically necessary boundary (GNB). The continuation of the current flow in this direction (with grain G remaining close to the anode end of the line) does not increase  $\text{FWHM}_\xi$  of the streak, indicating the absence of dislocation activity in this grain during the “near anode” period of the test.

To determine the orientation of the activated slip systems we have simulated the Laue streaks corresponding to the activated dislocation arrangements in grains F and G. In Fig.3, the experimental and simulated (331), (222) and (113) Laue streaks are shown for the grain F (left) and (224), (222) and (422) Laue streaks for grain G (right). Laue streaks are shown in reciprocal space in the sample basis. Although orientation of streaks is different in different grains the experimental and simulated streaks remain parallel to each other.

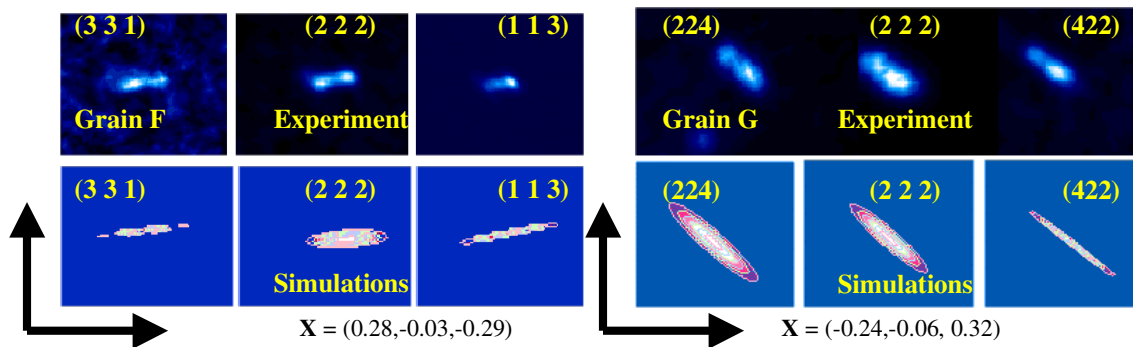


**Figure. 3** Experimental and simulated stereographic projections of different Laue streaks for grains F (left) and G (right). Simulations were performed for activated slip systems with Burgers vector  $\mathbf{b} = [\bar{1}01]$  and a dislocation line direction  $\tau = [1\bar{2}1]$  for F grain, and for two activated slip systems with  $\mathbf{b} = [011]$  and dislocation lines in directions  $\tau_1 = [2\bar{1}1]$  and  $\tau_2 = [2\bar{1}1]$  for a G grain.

Such peculiarities of plastic deformation in the “near anode/cathode” regions can be understood taking into account that Cu is preferentially depleted from the cathode region of the interconnect<sup>18, 19</sup>. Moreover the Al (0.5% wt. Cu) interconnect line in the initial

state might contain small ( $\sim 1.2\text{nm}$ ) precipitates of tetragonal  $\theta$  phase ( $\text{Al}_2\text{Cu}$ )<sup>18</sup>. The dissolution kinetics of this phase near the cathode end is coupling to the plastic deformation activity. Interestingly that during the time of electromigration test there is no visible dislocation activity close to the anode end of the line (as observed in this study), while the “near cathode” grain is quickly plastically deformed. To interpret such a behavior we expand the model of electromigration-induced Cu motion and precipitation in Al(Cu) interconnects, described in<sup>18</sup>, and take into account coupling between plastic deformation and precipitation formation and dissolution in different regions of the line. Presence of small precipitates is known to strengthen the Al-based alloys and increase their resolved shear stress. Cu depletion in the near cathode region causes dissolution of precipitates. Decrease of precipitates size first causes symmetric broadening of the Laue spot, as observed here (Fig.2b, curve2). After precipitates dissolve the critical shear decreases and plastic deformation is activated. This is accompanied with streaking and further splitting of Laue spots (Fig2b, curve 3). With the reverse of current flow Cu concentration in this grain starts to increase and precipitations form again. Critical shear stress increases in this grain and plastic activity stops (Fig. 2b, curves 4,5 ). The dislocation grouping in the wall is stable and is not destroyed by this process, however new dislocations do not appear. In the “near anode” grain F increase of Cu concentration slightly increases the size of precipitate (which slightly decreases the FWHM of the Laue spot (Fig. 1a, curves 2,3)). Critical shear stress is high and plastic activity is suppressed. Reversal of current flow is accompanied with dissolution of precipitates. Critical shear stress decreases and plastic deformation occurs (Fig. 2a, curves 4,5). This supports the idea<sup>18</sup> that Al(0.5% wt. Cu) interconnects are most reliable when Cu depletion from the cathode end is the slowest.

### **Geometrically necessary boundaries (GNBs) in the interconnect line**

We demonstrated that the evolution of the dislocation structure during electromigration is highly inhomogeneous and results in the formation of unpaired randomly distributed dislocations as well as geometrically necessary dislocation boundaries (GNBs). Analysis of dislocation structure from data taken with the white X-ray microdiffraction technique is based on the approach<sup>20-22</sup>. Here we extended the method to consider individual unpaired dislocations (GNDs for Geometrically Necessary Dislocations) within the scattering domains separated by geometrically necessary dislocation boundaries (GNB).

Consider deformation cells with different orientations in interconnect line separated by GNBs formed by unpaired tilt dislocation walls shown at Fig. 4. Each wall provides a rotation between two neighboring mosaic blocks around the direction of dislocation lines within the wall. The unit vector  $\omega$  parallel to the rotation axis of each wall coincides with the unit vector  $\tau$  along the dislocation lines in the case of a tilt boundary. We consider pure tilt boundaries formed by unpaired equidistant edge dislocations (so called “thin walls”<sup>16,22</sup>). Such boundaries does not produce any long-range strain but, only rotations. The remaining residual stresses in the boundary region are periodic with a wavelength  $b^* = bcsc\Theta/2$ . These stresses are only appreciable only at the distances less then  $b^*$  from the boundary<sup>13</sup>. If  $h$  is the distance between these dislocations in the wall, one can consider the boundary as a single defect producing the local rotation field. The misorientation angle  $\Theta$  due to such a boundary is defined by the equation

$b/h = 2\sin(\Theta/2)$ , where  $b/h \approx \Theta$  for small angle boundaries. We define the average size of the deformation cells  $D^+$  between the two neighboring GNBs. The total density of unpaired dislocations grouped in the walls is denoted by  $n^+ = \frac{1}{D^+h}$ . The mean deformation tensor results in pure rotations about the direction of dislocation lines in the wall. This tensor depends on the type and misorientation angles of one each GNB and their density.

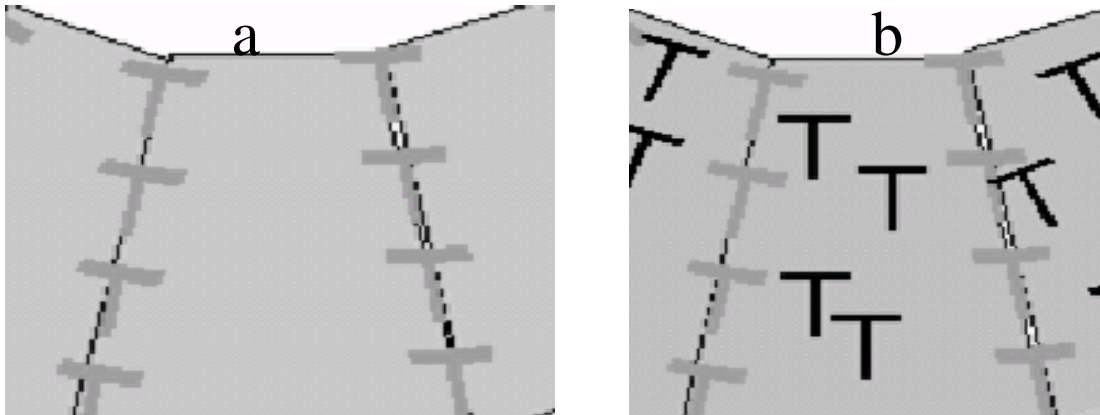


**Figure. 4** Scheme of the interconnect line with complete (a) and partial (b) grouping of unpaired dislocations within two geometrically necessary boundaries.

It is worth noting that the start of plastic activity in all grains corresponds to highly anisotropic intensity distribution along the streak with the maximum of intensity concentrated on one side of the streak and long “tail” with gradually decreasing intensity (Figs.2 a, curve 4; 2b curve 3; 2c curve 2). Such intensity distribution is related to the gradient of the dislocation density with depth<sup>21</sup>. This supports the model of dislocation climb from the interface into the depth of the interconnect line<sup>16,17,19</sup>.

## CONCLUSIONS

Our analysis of the orientation of the activated dislocation slip systems shows that in the middle of the interconnect line in the polycrystalline region the slip systems with dislocation lines almost parallel to the direction of current flow are activated first. Near the ends of the line plastic activity is coupled with the depletion of Cu from the cathode end of the line. There is practically no plastic activity in the “near anode” end of the line. Gradient of dislocation density with depth is observed. Coupling between the plastic activity and density of unpaired dislocations with the Cu depletion from the cathode and dissolution of precipitates during electromigration is demonstrated here for the first time.

## ACKNOWLEDGEMENT

Research is supported by the Director, Office of Science, Office of Basic Energy Sciences, U.S. Department of Energy, under Contract DE-AC05-00OR22725 with UT-Battelle, LLC and with the Advanced Light Source, Materials Science Division, under the Contract No. DE-AC03-76SF00098 at Lawrence Berkeley National Laboratory.

## REFERENCES

- <sup>1</sup> I.A. Blech, J. Appl. Phys., **47**, 1203 (1976).
- <sup>2</sup> C.V. Thompson and J.R. Lloyd, Mater. Res. Soc., Bull. **18**, 19 (1993).
- <sup>3</sup> M.A. Korhonen, P. Borgesen, K.N. Tu, and C.-Y. Li, J. Appl. Phys. **73**, 3790 (1993).
- <sup>4</sup> N. Tamura, A.A. MacDowell, R.S. Celestre, H.A. Padmore, B.C. Valek, J.C. Bravman, R. Spolenak, W.L. Brown, T. Marieb, H. Fujimoto, B.W. Batterman and J.R. Patel, Appl. Phys. Lett. **80**, 3724 (2002).
- <sup>5</sup> N. Tamura; R. Spolenak, B.C. Valek; A. Manceau; M. Meier Chang; R.S. Celestre; A.A. MacDowell; H.A. Padmore and J.R. Patel; Review of Scientific Instruments **73**, 1369 (2002) .
- <sup>6</sup> A.A.MacDowell, R.S.Celestre, N.Tamura, R.Spolenak, B.C. Valek, W.L.Brown, J.C.Bravman, H.A.Padmore, B.W.Batterman and J.R.Patel, Nuclear Instruments and Methods in Physics Research A **467-468**, 936 (2001).
- <sup>7</sup> G.E. Ice and B. C. Larson, Advanced Engineering Materials, **2**, 10, 643 (2002).
- <sup>8</sup> B.C.Larson, Wenge Yang, G.E.Ice, J.D.Budai and J.Z.Tischler, Nature, **415**, 887 (2002).
- <sup>9</sup> P.-C. Wang, I. C. Noyan, S. K. Kaldor, J. L. Jordan-Sweet, E. G. Liniger, and C.-H. Ku, Appl. Phys. Lett., **78**, 2712 (2001).
- <sup>10</sup> P. C. Wang, G. S. Cargill III, I. C. Noyan, C. K. Hu, Appl. Phys. Lett., **72**, 1296 (1998).
- <sup>11</sup> N. Tamura, J.-S. Chung, G.E. Ice, B.C. Larson, J.D. Budai, J.Z. Tischler, M. Yoon, E.L. Williams, and W.P. Lowe, Mater. Res. Soc. Symp. Proc., **563**, 175 (1999).
- <sup>12</sup> N. Tamura, B. C. Valek, R. Spolenak, A. A. MacDowell, R. S. Celestre, H.A.Padmore, W. L. Brown, T. Marieb, J. C. Bravman, B. W. Batterman and J. R. Patel, Mat. Res. Soc. Symp. Proc., **612**, D.8.8.1 (2001) .
- <sup>13</sup> R. Spolenak, D.L. Barr, M.E. Gross, K. Evans-Lutherodt, W.L. Brown, N. Tamura, A.A. MacDowell, R.S. Celestre, H.A.Padmore, J.R. Patel, B.C. Valek, J.C. Bravman, P. Flinn, T. Marieb, R.R. Keller, B.W. Batterman, Mater. Res. Soc. Symp. Proc., **612**, D10.3.1 (2001).
- <sup>14</sup> B.C. Valek, N. Tamura, R. Spolenak; A.A. MacDowell; R.S. Celestre; H.A. Padmore; J.C. Bravman; B.W. Batterman; J.R. Patel, Mat. Res. Soc. Symp. Proc. **673**, P7.7.1 (2001).
- <sup>15</sup> B.C. Valek, N. Tamura, R. Spolenak, J.C. Bravman, A.A. MacDowell, R.S. Celestre, H.A. Padmore, W.L. Brown, B.W. Batterman and J.R. Patel, Appl. Phys. Lett. **81**, 4168 (2002).
- <sup>16</sup> R.I. Barabash, G.E. Ice, N. Tamura, B.C. Valek, J. C. Bravman, R. Spolenak and J.R. Patel, J. Appl. Physics, **93**, 5701 (2003).
- <sup>17</sup> R.I. Barabash, G.E. Ice, N. Tamura, B.C. Valek, J. C. Bravman, R. Spolenak and J.R. Patel, Mater.Res.Soc.Symp.Proc.,**738**, (2003).
- <sup>18</sup> C. Witt, C. Volkert, E. Arzt, Acta Materialia, **51**, 49 (2003) .
- <sup>19</sup> R. Spolenak, O. Kraft, and E. Arzt, AIP. Con. Proc., **491**, 126 1999.
- <sup>20</sup> R. Barabash, G.E. Ice, B.C. Larson, G.M. Pharr, K.-S. Chung, W. Yang, Appl.Phys.Lett., **79**, 749, (2001).
- <sup>21</sup> R. Barabash, G. Ice, in press.
- <sup>22</sup> R. Barabash, G.E. Ice, F. Walker, J. Appl. Physics, **93**, 3, 1457 (2003)